metals

MDPI

Article

Study on the Thermal Conductivity Characteristics of Graphene Prepared by the Planetary Ball Mill

Gwi-Nam Kim, Ji-Hye Kim, Bo-Sung Kim, Hyo-Min Jeong and Sun-Chul Huh *

Department of Energy and Mechanical Engineering, Gyeongsang National University, Cheondaegukchi-Gil 38, Tongyeong 53064, Gyeongnam, Korea; rnlska0717@nate.com (G.-N.K.); wlgp1302@naver.com (J.-H.K.); mplusw35@naver.com (B.-S.K.); hmjeong@gnu.ac.kr (H.-M.J.)
* Correspondence: schuh@gnu.ac.kr; Tel.: +82-55-772-9111

Academic Editor: Chun-Liang Chen
Received: 16 August 2016; Accepted: 26 September 2016; Published: 29 September 2016

Abstract: This study was designed to examine the physical disintegration of graphene (GN), an excellent heat conductor, by using the planetary ball mill, a simple and convenient means to produce particles arbitrarily. The conditions for the disintegration of GN were distinguished by the rotation of the planetary ball mill (200 rpm, 400 rpm, and 600 rpm) and by the duration of its operation (30 min, 60 min, and 90 min), respectively. From the results, we saw that, when experimental conditions are 200 rpm with 60 min, the particle size was the smallest (at 328 nm) and the results of thermal conductivity were the highest. In the absorbance results, GN was well dispersed because the value of its absorbance is high.

Keywords: nano fluid; graphene; planetary ball mill; disintegration; particle size; thermal characteristic

1. Introduction

Nano-fluid refers to the new concept of pure heat transferring fluids in which the nm sized solid particles of excellent heat conductivity are dispersed stably. Owing to its excellent heat conductive property, it is expected to be a heat exchanging medium for the next generation [1,2]. The nano-sized powders of copper [3], copper oxide [4], titanium oxide [5], aluminum oxide [6], and carbon nanotube (CNT) [7–9], the heat conductivities of which are higher than general fluids are prepared and dispersed into such fluid to achieve an improved efficiency of heat conductivity. Recently, the graphene (GN) [10–15] of high heat conductivity has been focused upon as one of the nano-sized particles that can be added to such nano-fluids.

GN is a novel carbon nanomaterial with excellent electronic, mechanical, and thermal properties. The thermal conductivity of GN is as large as around 5000 W/m K, which makes it the most promising nanoadditive for nanofluids [16].

However, nanofluid with GN and CNT have faced obstacles such as bad dispersibility of particles, sedimentation of particles and erosion of equipment. K. Wusiman et al. [7] have shown that CNT nanofluid was made with sodium dodecyl sulfate (SDS) and sodium dodecylbenzene sulfonate (SDBS). Therefore, dispersibility surely increases. However thermal conductivity of nanofluid with surfactant is lower than distilled water, to its thermal performance is not good as that of enhanced nanofluid. Therefore, the application of surfactants is not appropriate for use on the allotropes of carbon as GN and CNT, and research on improving thermal performance without surfactant is certainly necessary.

This study was designed to examine the physical disintegration of GN, an excellent heat conductor, by using the planetary ball mill, a simple and convenient means to produce particles arbitrarily. The conditions for the disintegration of GN were distinguished by the rotation of the planetary ball mill (200 rpm, 400 rpm, and 600 rpm) and by the duration of its operation (30 min, 60 min, and 90 min).

The GN that disintegrated respectively according to each combination of above conditions was then used for the preparation of corresponding nano-fluids to examine respective thermal properties.

2. Equipment and Materials

2.1. Materials

The physical properties of the GN used in this study (Supplier: Graphene Supermarket, Suffolk County, NY, USA) were 100 of the specific surface area and 99.9% of the purity. The average thickness of the GN was 8 nm, and the average particle size (cross direction) was ~550 nm (150~3000 nm).

2.2. Ultrasonic Generator

Figure 1 is an illustration of the schematic diagram of the ultrasonic generator (1510E-DTH, Branson Ultrasonic Corporation 41, Danbury, CT, USA). The GN, the carbon allotrope like the carbon nanotube, precipitates by the coagulation attributable to the Van der Waals force therein. Thus, the simple mixing of GN into basic fluid does not result in complete dispersion and thereby the fluid does not exhibit the significant thermal property of the GN. Therefore, in this study, the ultrasonic generator was used to secure the stabilized dispersion of the GN nano-fluid based on distilled water.

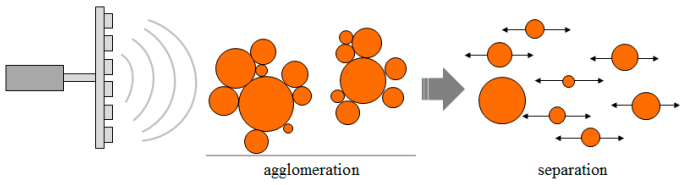

Figure 1. Schematic diagram of ultrasonic generator.

2.3. Analysis Methods

Figure 2 shows the measuring equipment used in this study. The instrument measuring the particle size distribution (PSD, Zetasizer, Nano-S90, Malvern Instruments Ltd., Malvern, UK) in Figure 2a was also used to measure the degree of particle dispersion which varied according to different numbers of rotations per minute and durations of disintegration. The thermal conductivity of the distilled water based GN nano-fluid that was put under the room temperature ranged from 20 °C to 40 °C. It was measured by using the measurement device (LAMBDA, F5 Technologie GmbH, Willingshausen, Germany) as shown in Figure 2b employing the transient hot-wire method that varied the temperature thereof by the spacing of 4 °C. In addition, the samples of nano-fluid were visualized after a duration of 15 days to check the precipitation of GN therein. Transmission electron microscope (TEM) analysis was JEOL JEM2010 (JEOL Ltd., Tokyo, Japan) as shown in Figure 2c to investigate the morphology of GN powders. Nanofluid was prepared by dispersing a known amount of GN in the base fluid by ultrasonication (20 min). The UV-vis spectrum (X-ma 3100 spectrophotometer operating between 200 and 1000 nm, Human Ltd., Seoul, Korea) as shown in Figure 2d was used. The samples were diluted up to the extent that they were suitable for UV-vis measurements. One hour before the measurement, the UV spectrometer was turned on to be warmed up. The GN-water nanofluids were poured into a 1 cm quartz cuvette.

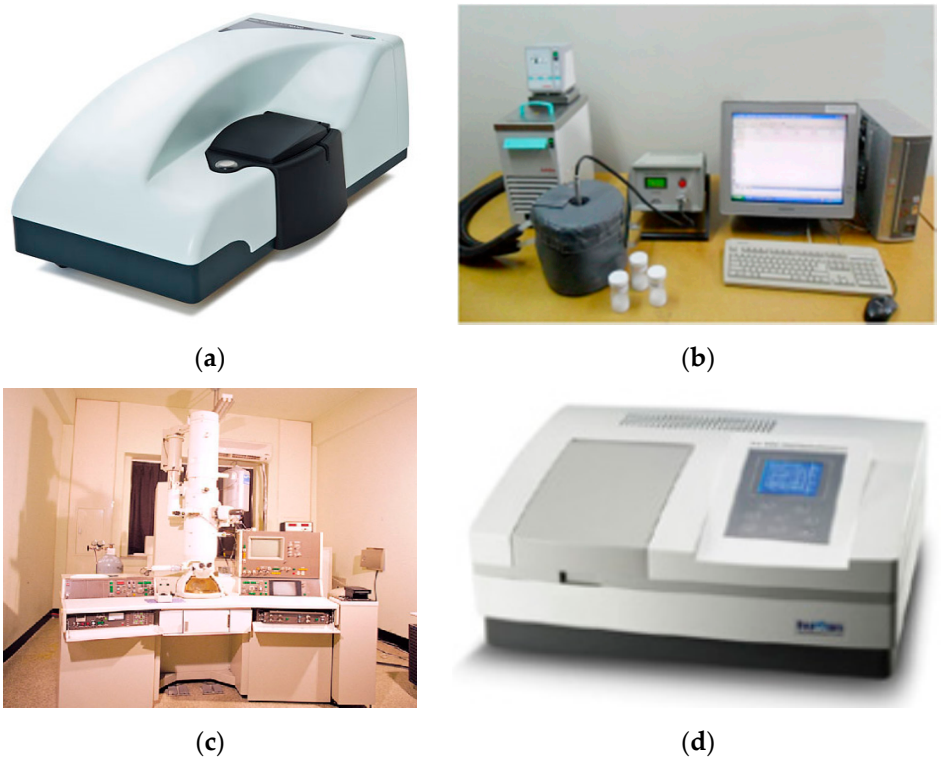

Figure 2. Photograph of measurement equipments. (**a**) Zetasizer, Nano590; (**b**) Thermal Conductivity measuring system LAMBDA; (**c**) Transmission Electron Microscopy; (**d**) X-ma 3100.

3. Experimental Methods

In the process of disintegration of the GN by using the planetary ball mill, the number of rotations, duration of disintegration, charging amount and size of balls are the experimental variables most influential on the experimental results. The milling conditions under wet or dry environment also are significant experimental variables.

In general, the milling under the condition of a dry environment does not need post disintegration treatment. However, this would be disadvantageous in that it would leave coagulated particles of GN. In the case of the milling under the wet environment free from the coagulation of GN, the distilled water has to be completely vaporized, especially in cases of the disintegration of GN preserved with or mixed with other materials. The studies employing either the wet or the dry condition for the milling using the planetary ball mill have been carried out [17,18]. In this study, the condition of wet milling was selected for the disintegration of GN to attain the high degree of dispersion and thermal conductivity of disintegrated GN in the nano-fluid.

The experimental conditions applied to the disintegration of GN are summarized in Table 1. As the conditions were applied to the experiment, the number of rotations and the duration of disintegration were varied with the fixed conditions of the ball size (1 mm) and charged amount of balls (40%). The reason behind the selection of this combination of experimental conditions is based on the study conducted by Munkhbayar et al. [19] that employed respective ball sizes (1 mm, 3 mm, and 5 mm) and found that the highest thermal conductivity of GN disintegrated under the condition of the ball size of 1 mm. An excessive charge of balls into the container of disintegration would disturb the smooth disintegration of GN whereas the moderate charge of balls would deprive the balls of the chances of generating colliding impacts leading to the waste of energy. The experimental conditions were thus determined by taking the above into account.

Table 1. Ball milling condition of graphene (GN).

No.	Parameter	Value
1	Ball size	1 (mm)
2	Ball charge volume	40 (%)
3	Rotation speeds	200, 400, 600 (rpm)
4	Time	30, 60, 90 (min)
5	Condition	Wet

The disintegration container of the volume of 45 mL was employed for the experiment into which the abrasion resistant Zirconia balls were charged. The sampled amount of 0.1 g of the GN was put into the pot together with the balls according to each condition of experiment and then the wet disintegration proceeded. On completion of each process of disintegration, the respective distilled water based GN nano-fluids of 100 mL were prepared and then they were put into each vial.

4. Results and Discussion

4.1. Results of PSD Measurement

Figure 3 illustrates the results of the PSD measurements obtained from samples of the disintegrated GN according to each predetermined experimental condition. The measurement of average particle size of the original raw GN was 1087.2 nm. This was reduced to 479.2 nm, 412.2 nm, and 440.7 nm by the disintegration, which lasted for 30 min. The measurements were 328.2 nm, 518.7 nm, and 715 nm after the disintegration continued for 60 min. The 90 min of the duration of disintegration yielded the measurements of average particle size of 557.2 nm, 666.4 nm, and 757.5 nm.

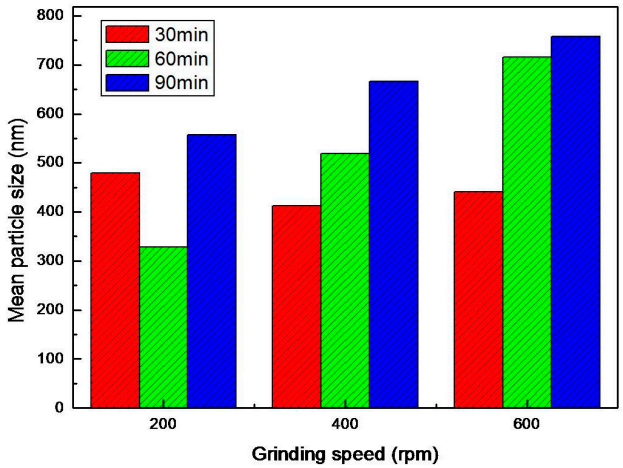

Figure 3. Influence of Experimental parameters on the mean particle size of GN structure.

The average particle size of GN that resulted from each duration of disintegration tended to increase along with the increased number of rotations. It was estimated that this would be attributable to the weight of the 1 mm balls being too light and thereby causing the balls to be attached onto the inner wall of the pot by the centrifugal force during the rotation of very high speed, which could cause excessive vibration and noise from the equipment.

In terms of the duration of disintegration, the average particle size of GN tended to increase proportionally to the length of duration. The smallest average particle size of GN resulted from the conditions of 400 rpm and 30 min of the duration of disintegration. The following combinations of experimental conditions of 200 rpm with 60 min and 200 rpm with 90 min of the duration of disintegration were also applied, and they rendered similar small average particle sizes of the GN.

The condition comprised the ball size of 1 mm and 200 rpm of rotation was concluded that it realized the smooth disintegration of GN.

Thereby, the disintegration of GN attained through the operation of planetary ball mill rendered significant decrease in average particle size of the GN compared to its original ones and the resulted increase in the specific surface area thereof gave us the promising high thermal conductivity.

4.2. Measurements of Thermal Conductivity

Figure 4 shows the graph comparing the standard values presented in the reference [20] with the measurements of thermal conductivity of distilled water. The thermal conductivity of distilled water was measured to calibrate the measuring equipment in advance of the measurement of thermal conductivity of prepared nano-fluids. As represented in Figure 5, the measurements of thermal conductivity of distilled water approximated to the standard values with the error rate less than 1%.

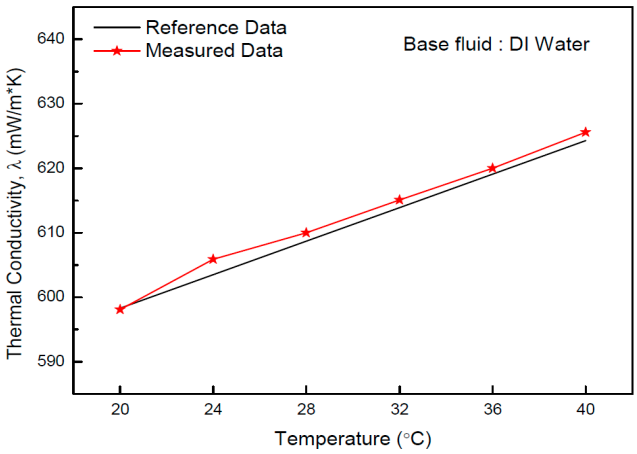

Figure 4. The measured thermal conductivity for the base fluid.

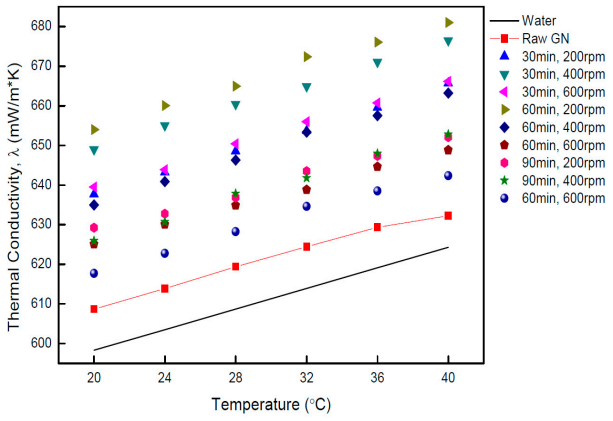

Figure 5. The thermal conductivity of GN solutions prepared by various parameter.

Figure 5 shows the graph of the measurements of thermal conductivities of nano-fluids prepared from each condition. The thermal conductivity of original GN was higher than that of distilled water but it became lower than that of the disintegrated GN. The causes of this result were estimated to possibly be the coagulation and big particle size of GN and its irregular dispersion. The particles size was influenced by grinding through the ball mill as shown in Figure 3, the small particles seemed to have high thermal conductivity due to increasing surface area. As a result, GN nano fluid was confirmed to be able to increase thermal performance by controlling particle size without surfactant and functionalization. The thermal conductivity of nano-fluids increases linearly along with the

increase in overall temperature. This enhancement mechanism is explained by the brown motion being dependent on fluid temperature and so the huge enhancement in thermal conductivity with temperature is quite explicable [21].

Figure 6a represents the measurements of thermal conductivity of nano-fluids that resulted from the experimental conditions of the duration of 30 min of disintegration with varied numbers of rotations. The highest thermal conductivity resulted from the 400 rpm of rotation similar to those obtained from the conditions of 200 rpm and 600 rpm of rotation.

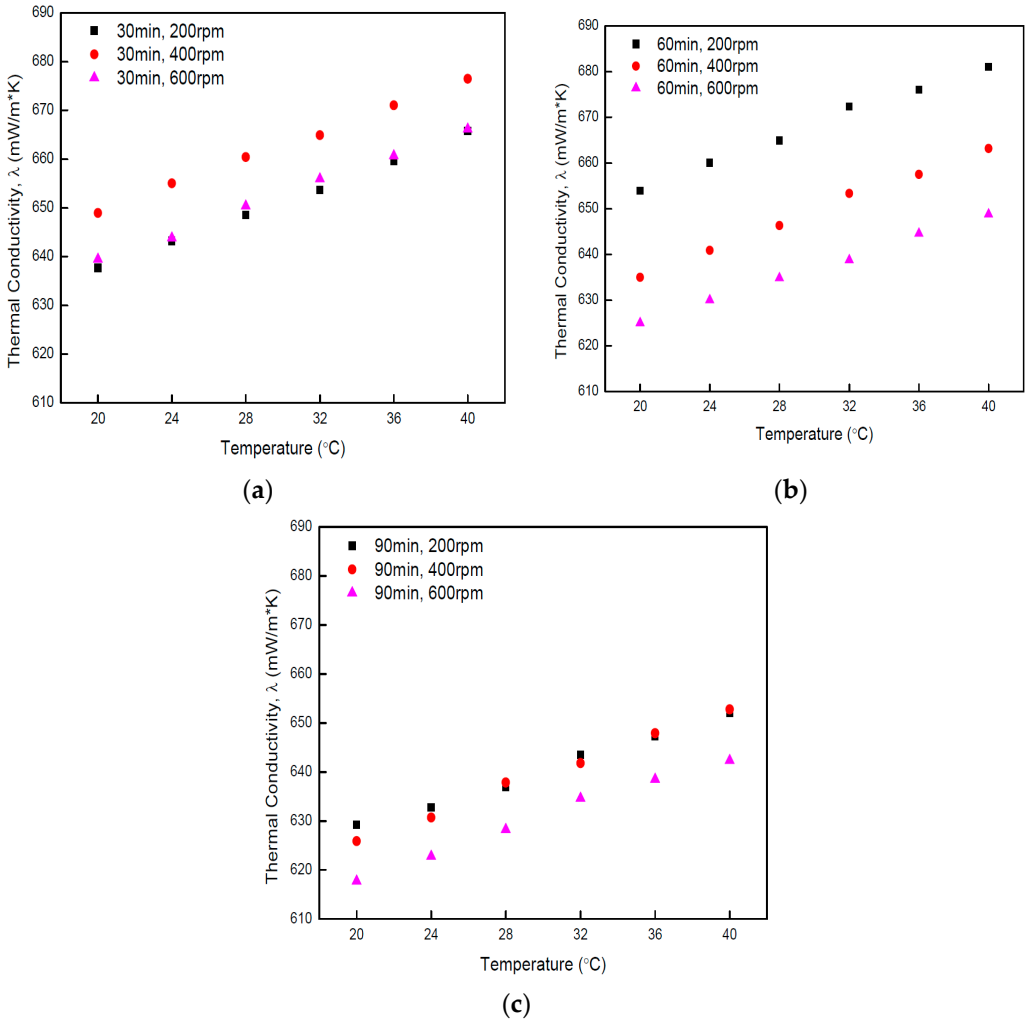

Figure 6. The thermal conductivity measurement value of the changes in the grinding time. (**a**) Grinding time: 30 min; (**b**) Grinding time: 60 min; (**c**) Grinding time: 90 min.

Figure 6b is a representation of the measurements of thermal conductivity of nano-fluids resulted from the experimental conditions of the duration of 60 min of disintegration with varied numbers of rotations. In contrast to the result of the 30 min duration of disintegration, the measurements varied significantly depending on the changed numbers of rotations. The highest thermal conductivity resulted from the condition of 200 rpm of rotation from the sample with identical conditions to that which rendered the smallest average particle size of GN represented in Figure 4. Thereby, the inverse proportionality of the average particle size of GN to its degree of thermal conductivity was identified.

Figure 6c shows the graph of the measurements of thermal conductivity of nano-fluids resulting from the experimental conditions of the duration of 90 min of disintegration with varied numbers of rotations. The measurements appear to be higher than the thermal conductivities of distilled water and

GN. However, they are roughly lower than those that resulted from the durations of the disintegration of 30 min and 60 min. This implies that an excessive disintegration of GN beyond a certain limit could bring about adverse effects.

By taking the PSD measurements represented in Figure 4 and taking the measurements of thermal conductivity represented in Figures 6 and 7 into account, we identified that the thermal conductivity increases in inverse proportionally to the size of particles. This is the well-known relationship between the lower level of particle size corresponding to higher level of thermal conductivity [22].

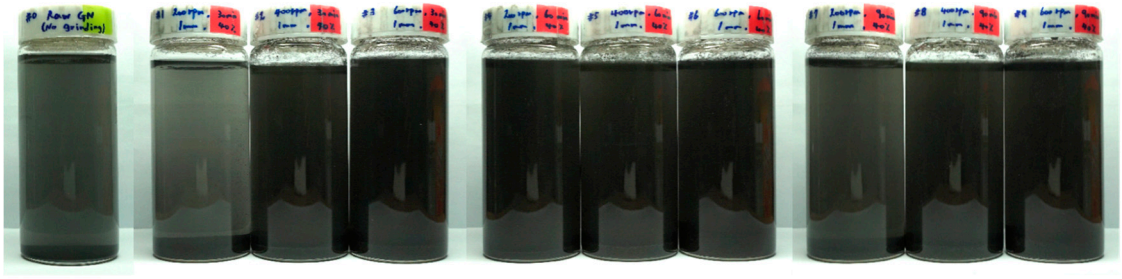

Figure 7. Dispersion result of GN nanofluid during 15 days.

The Brunauer-Emmett-Teller (BET) specific surface area increase in accordance with decreased particle size should also be taken into account for the interpretation of this result [23].

4.3. Result of Precipitation of Disintegrated GN

Figure 7 shows the visualization of GN particles disintegrated according to each combination of experimental conditions and then precipitated for 15 days in the equivalent amount of nano-fluid samples. The nano-fluids were ultrasonically treated for 30 min for the dispersion of GN particles therein and were each preserved in 100 mL vials.

The visualized results show the significant precipitation of GN particles in each nano-fluid. The suspension of the original raw GN showed rapid precipitation of GN in less than 24 h duration owing to its strong coagulation. In contrast, the suspension that contained the disintegrated GN showed slow precipitation and resulted in the uniform dispersion of disintegrated GN particles after 24 h of duration.

For the disintegration of GN, the sole application of the mechanical method seems unable to maintain the long duration of dispersion. Thereby, the chemical methods employing surfactants that could change surface properties of nanoparticles as a stable dispersant are also used to keep the state of dispersion of (floating) nanoparticles [24].

The addition of a moderate amount of surfactant may improve the dispersion of nanoparticles whereas an excessive application of surfactant could bring about the degradation in viscosity, thermal characteristics, and chemical stability of the nano-fluid [7].

4.4. UV-Vis Spectrum

UV-vis spectrophotometer analysis is a convenient approach to characterize the stability of colloids quantitatively [24]. If absorbance is high, dispersibility and thermal conductivity is increased because GN is equably dispersed.

The UV-vis spectrum as shown in Figure 8 of GN dispersion in distilled water is featureless with a monotonic decrease in absorbance with increasing wavelength, except for below 270 nm, where a strong absorption band is observed. Figure 8a is a graph of absorbance following rotation speed during 30 min. The result of the 600 rpm test is higher than the other results, followed by 400 rpm, 200 rpm. In the case of 200 rpm, the substance is too poorly grinded due to short working time and slow rotation speed. Figure 8b is a graph of absorbance during 60 min. The result of the 200 rpm test is

the highest, and the 400 rpm and 600 rpm cases show similar results. Compared with trend of thermal conductivity in Figure 7b, the results are very similar. Figure 8c is graph of absorbance during 90 min. The more the rotation speed decreases, the more absorbance increases. This result shows a similar trend compared with results of thermal conductivity in Figure 8c. After considering all the results, the more that working time is shortened and rotation speed is slowed, the smaller the particle size of GN due to an effective crush. The smaller the particle size is, the more dispersibility and thermal conductivity were improved.

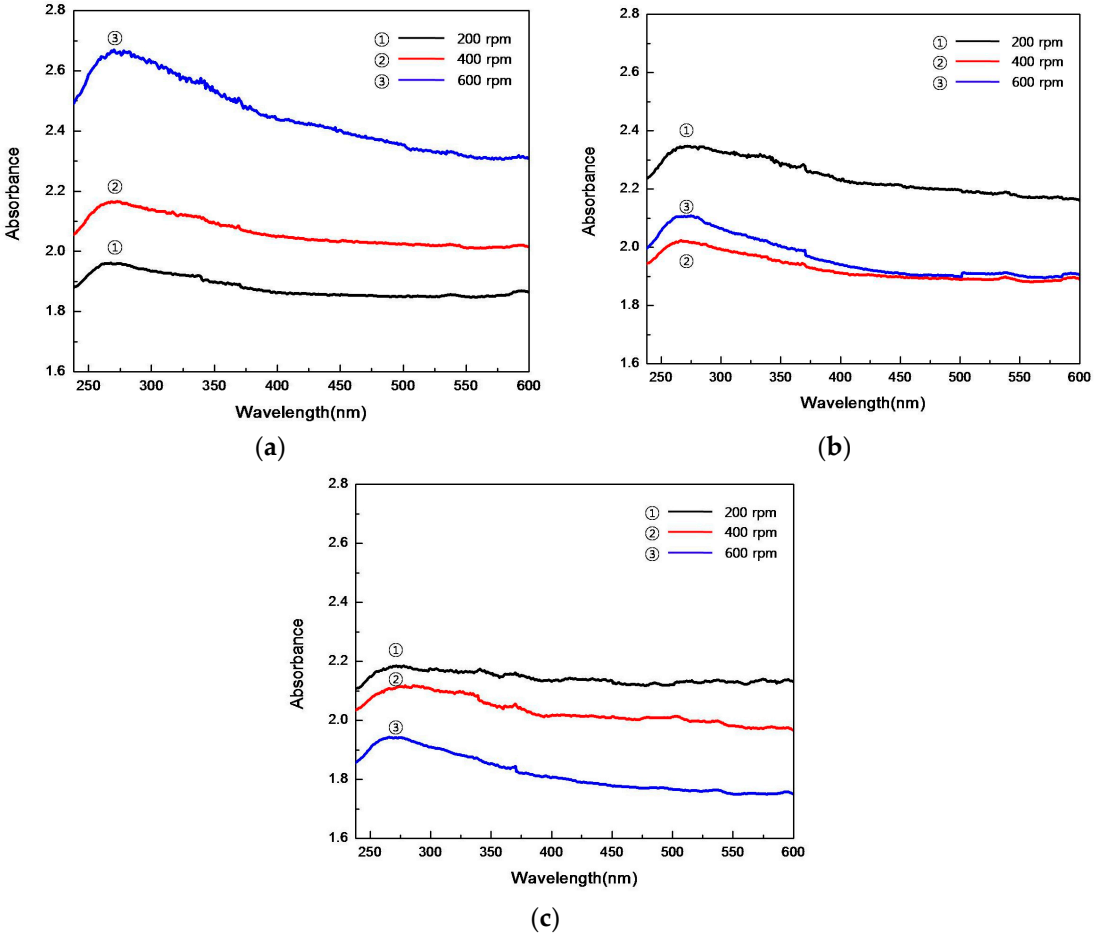

Figure 8. The graph of Absorbance measurement of the changes in the grinding time. (**a**) Grinding time: 30 min; (**b**) Grinding time: 60 min; (**c**) Grinding time: 90 min.

4.5. Result of TEM Measurement

Figure 9 shows the TEM image of the original GN used in this study. As shown in the picture, the 2-dimensional structured GN appears in flat and wide planar shape. The GN particles coagulated by the Van der Waals force can also be identified.

Figure 10 is an image of GN particles disintegrated by the planetary ball mill. In contrast with the original GN, the disintegrated particles of GN separated from each other can be seen. The increased specific surface area (BET) that resulted was concluded to have contributed to the improvement in thermal conductivity.

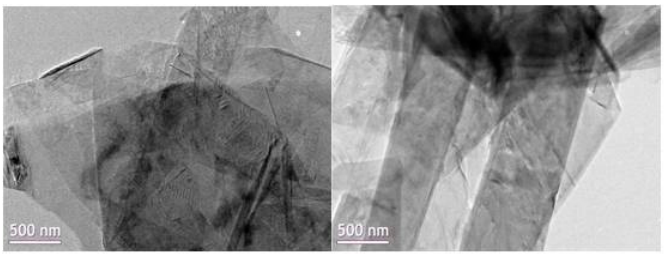

Figure 9. Transmission electron microscope (TEM) images of the raw GN.

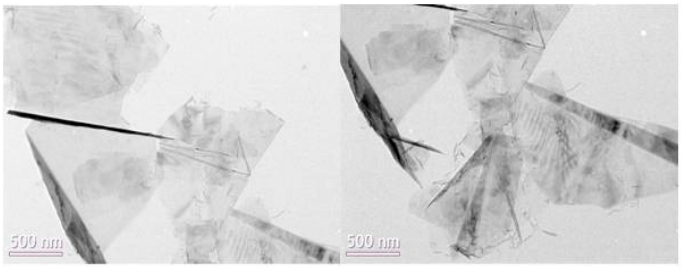

Figure 10. TEM images of the ground GN.

5. Conclusions

In this study, the planetary ball mill was used to disintegrate the GN by varying the duration of disintegration and the number of rotations in the operation of the planetary ball mill. The disintegrated GN particles were then used to prepare nano-fluids in which the disintegrated GN particles were dispersed to examine the resulted thermal conductivity of nano-fluids through transient hot-wire method. The degree of precipitation of disintegrated GN particles dispersed in each sample of nano-fluids was visualized and the TEM images of disintegrated GN particles in a dispersed state were captured. The conclusions obtained are summarized below:

(1) Through the process of the disintegration of GN particles, the average particle size of GN decreased and the minimum average particle size of GN was realized from the combination of experimental conditions of 90 min duration of disintegration and 200 rpm of the operation of the planetary ball mill. In contrast, the combined experimental conditions of 90 min duration of disintegration and 600 rpm of the operation of planetary ball mill yielded the biggest average particle size of GN. The cause of these results was attributed to the light weight of the balls (1 mm) attached onto the inner wall of the pot of planetary ball mill by the centrifugal force induced by the high speed rotation that eventually caused the disturbed impact collisions of balls that were supposed to cause the disintegration of GN particles.

(2) The measurements of thermal conductivity of nano-fluids prepared in this study appeared similar than those of PSD measurements from which the inverse proportionality of average size of particles dispersed in nano-fluid to the level of thermal conductivity of corresponding nano-fluid was identified. The disintegrated GN seen from the captured TEM image showed the average particle size to be smaller than that of the original GN with less coagulation. Thereby, the increased thermal conductivity of nano-fluids was concluded to potentially be attributable to the increased specific surface area of GN particles that resulted from the disintegration that decreased the average particle size.

(3) The degree of precipitation of disintegrated GN particles dispersed in each sample of nano-fluids was visualized according to varied duration of precipitation. An additional application of surfactant to the disintegration of GN particles beyond the sole application of the mechanical method could also improve the degree of dispersion of disintegrated GN particles.

Acknowledgments: This work was supported by the Gyeongsang National University Fund for Professors on Sabbatical Leave (2014) and Basic Science Research Program through the National Research Foundation of Korea (NRF) funded by the Ministry of Science, ICT and future Planning (2015R1A2A2A01004579).

Author Contributions: All the authors contributed equally to this research activity. Drafting of manuscript: Gwi-Nam Kim; All of test: Gwi-Nam Kim and Ji-Hye Kim and Bo-Sung Kim; Planning and supervision of the research: Hyo-Min Jeong and Sun-Chul Huh.

Conflicts of Interest: The authors declare no conflict of interest.

References

1. Das, S.K.; Choi, S.U.; Yu, W.; Pradeep, T. *Nanofluids: Science and Technology*; John Wiley & Sons: Hoboken, NJ, USA, 2007.
2. Choi, S. Enhancing thermal conductivity of fluids with nanoparticles. *ASME Publ. FED* **1995**, *231*, 99–106.
3. Kole, M.; Dey, T.K. Thermal performance of screen mesh wick heat pipes using water-based copper nanofluids. *Appl. Therm. Eng.* **2013**, *50*, 763–770. [CrossRef]
4. Swadzba-Kwasny, M.; Chancelier, L.; Ng, S.; Manyar, H.G.; Hardacre, C.; Nockemann, P. Facile in situ synthesis of nanofluids based on ionic liquids and copper oxide clusters and nanoparticles. *Dalton Trans.* **2012**, *41*, 219–227. [CrossRef] [PubMed]
5. Buschmann, M.H.; Franzke, U. Improvement of thermosyphon performance by employing nanofluid. *Int. J. Refrig.* **2014**, *40*, 416–428. [CrossRef]
6. Khoshvaght-Aliabadi, M. Influence of different design parameters and Al_2O_3-water nanofluid flow on heat transfer and flow on heat transfer and flow characteristics of sinusoidal corrugated channels. *Energy Convers. Manag.* **2014**, *88*, 96–105. [CrossRef]
7. Wusiman, K.; Jeong, H.; Tulugan, K.; Afrianto, H.; Chung, H. Thermal performance of multi-walled carbon nanotubes (MWCNTs) in aqueous suspensions with surfactants SDBS and SDS. *Int. Commun. Heat Mass Transf.* **2013**, *41*, 28–33. [CrossRef]
8. Amri, A.; Sadri, R.; Ahmadi, G.; Chew, B.; Kazi, S.; Shanbedi, M. Synthesis of polyethylene glycol-functionalized multi-walled carbon nanotubes with a microwave-assisted approach for improved heat dissipation. *RSC Adv.* **2015**, *5*, 35425–35434. [CrossRef]
9. Ghiadi, B.; Baniadam, M.; Maghrebi, M.; Amiri, A. Rapid, one-pot synthesis of highly-soluble carbon nanotubes functionalized by L-arginine. *Russ. J. Phys. Chem. A* **2013**, *87*, 649–653. [CrossRef]
10. Amiri, A.; Sadri, R.; Shanbedi, M.; Ahmadi, G.; Chew, B.T.; Kazi, S.N.; Dahari, M. Performance dependence of thermosyphon on the functionalization approaches: An experimental study on thermo-physical properties of graphene nanoplatelet-based water nanofluids. *Energy Convers. Manag.* **2015**, *92*, 322–330. [CrossRef]
11. Mehrali, M.; Sadeghinezhad, E.; Latibari, S.T.; Kazi, S.N.; Mehrali, M.; Zubir, M.N.B.M.; Metselaar, H.S.C. Investigation of thermal conductivity and rheological properties of nanofluids containing graphene nanoplatelets. *Nanoscale Res. Lett.* **2014**, *9*, 1–12. [CrossRef] [PubMed]
12. Hajjar, Z.; Rashidi, A.M.; Ghozatloo, A. Enhanced thermal conductivities of graphene oxide nanofluids. *Int. Commun. Heat Mass Transf.* **2014**, *57*, 128–131. [CrossRef]
13. Wang, F.; Han, L.; Zhang, Z.; Fang, X.; Shi, J.; Ma, W. Surfactant-free ionic liquid-based nanofluids with remarkable thermal conductivity enhancement at very low loading of graphene. *Nanoscale Res. Lett.* **2012**, *7*, 1–7. [CrossRef] [PubMed]
14. Baby, T.T.; Ramaprabhu, S. Enhanced convective heat transfer using graphene dispersed nanofluids. *Nanoscale Res. Lett.* **2011**, *6*, 1–9. [CrossRef] [PubMed]
15. Yarmand, H.; Gharehkhani, S.; Ahmadi, G.; Shirazi, S.F.S.; Baradaran, S.; Montazer, E.; Zubir, M.N.M.; Alehashem, M.S.; Kazi, S.N.; Dahari, M. Graphene nanoplatelets-silver hybrid nanofluids for enhanced heat transfer. *Energy Convers. Manag.* **2015**, *100*, 419–428. [CrossRef]
16. Balandin, A.A.; Ghosh, S.; Bao, W.; Calizo, I.; Teweldebrhan, D.; Miao, F.; Lau, C.N. Superior thermal conductivity of single-layer graphene. *Nano Lett.* **2008**, *8*, 902–907. [CrossRef] [PubMed]
17. Kotake, N.; Kuboki, M.; Kiya, S.; Kanda, Y. Influence of dry and wet grinding conditions on fineness and shape of particle size distribution of product in a ball mill. *Adv. Powder Technol.* **2011**, *22*, 86–92. [CrossRef]
18. Feng, D.; Aldrich, C. A comparison of the flotation of ore from the Merensky Reef after wet and dry grinding. *Int. J. Miner. Process.* **2000**, *60*, 115–129. [CrossRef]

19. Munkhbayar, B.; Bat-Erdene, M.; Sarangerel, D.; Ochirkhuyag, B. Effect of the collision medium size on thermal performance of silver nanoparticles based aqueous nanofluids. *Compos. Part B Eng.* **2013**, *54*, 383–390. [CrossRef]
20. Lide, D.R. *CRC Handbook of Chemistry and Physics*, 89th ed.; CRS Press: Boca Raton, FL, USA, 2008; pp. 2–6.
21. Jang, S.P.; Choi, S.U. Role of Brownian motion in the enhanced thermal conductivity of nanofluids. *Appl. Phys. Lett.* **2004**, *84*, 4316–4318. [CrossRef]
22. Mahbubul, I.M.; Fadhilah, S.A.; Saidur, R.; Leong, K.Y.; Amalina, M.A. Thermophysical properties and heat transfer performance of Al_2O_3/R-134a nanorefrigerants. *Int. J. Heat Mass Transf.* **2013**, *57*, 100–108. [CrossRef]
23. Rahman, I.A.; Vejayakumaran, P.; Sipaut, C.S.; Ismail, J.; Chee, C.K. Size-dependent physicochemical and optical properties of silica nanoparticles. *Mater. Chem. Phys.* **2009**, *114*, 328–332. [CrossRef]
24. Li, X.; Chen, Y.; Mo, S.; Jia, L.; Shao, X. Effect of surface modification on the stability and thermal conductivity of water-based SiO_2-coated graphene nanofluid. *Thermochim. Acta* **2014**, *595*, 6–10. [CrossRef]